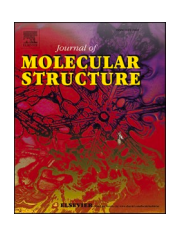
ELSEVIER

Contents lists available at ScienceDirect

Journal of Molecular Structure

journal homepage: www.elsevier.com/locate/molstr





Biocatalyst mediated green approach for 1,8-dioxo-octahydroxanthenes: SCXRD, Hirshfeld analysis and DFT studies as inhibitors of HIV reverse transcriptase

Swati R. Hoolageri ^a, Ravindra R. Kamble ^{a,*}, Aravind R. Nesaragi ^{a,b}, H.C. Devarajegowda ^c, Manojna R. Nayak ^a, Tukaram V. Metre ^a, Shrinivas D. Joshi ^d, Roopadevi P ^c, Vindu Vahini M ^e

- ^a Department of Studies in Chemistry, Karnatak University, Dharwad 580003, India
- ^b Department of Chemistry, Indian Institute of Technology, Dharwad 580007, Karnataka, India
- ^c Yuvaraja's College, University of Mysore, Mysuru 570005, Karnataka, India
- d Novel Drug Design and Discovery Laboratory, Department of Pharmaceutical Chemistry, S.E.T.'s College of Pharmacy, Dharwad 580002, India
- ^e Maharani's Science College for Women (Autonomous), Mysuru 570005, India

ARTICLE INFO

Keywords: In silico, HIV-AIDS Green synthesis 1,8-dioxooctahydroxanthenes Single crystal XRD DFT studies

ABSTRACT

AIDS, caused by human immunodeficiency virus (HIV) is persistent on being one among the deadliest disease of all time. It destroys the immune system of the body and there is currently no effective cure for this. In this regard, in continuation to our studies on green catalysts, more efficient, constructive, and environmentally sustainable protocols for the synthesis of xanthene and its derivatives as HIV Reverse Transcriptase inhibitors were developed with the use of biocatalyst *via* baker's yeast that explores a viable approach on expanding environmental challenges and enlightens the superiority and exclusivity of this protocol. The current approach manifests numerous notable advantages that include ease of preparation, handling and benignity of the catalyst, low cost, green reaction conditions, facile workup, excellent yields (87–96 %) with extreme purity. The title compounds were docked on the crystal structure of a catalytic complex of HIV-1 reverse transcriptase (PDB: 1RTD). The C-score values achieved in the range 6.68–3.05 suggest that docking analysis was propitious signifying the review of all the forces of interaction between the ligand and the protein. The crystal studies and DFT analysis of compound 3d correlate the optimized geometrical features with empirically accessible XRD data.

1. Introduction

HIV and AIDS (acquired immune deficiency syndrome) are topics of discussion in our day to day life now. AIDS is a chronic, potentially lethal illness caused by the human immunodeficiency virus (HIV). It belongs to the Lentivirus species that infects humans and is a subgroup of retroviruses. In due course it leads to AIDS, a disease in which the immune system gradually fails, permitting potentially fatal opportunistic infectivity and cancers to proliferate [1]. Scientists from across the globe have been researching AIDS for decades since it initially emerged in the early 1980's. Over time, researchers have made significant progress with regard to understanding and controlling the illness. Considering that it is predominantly a sexually transmitted disease, HIV/AIDS entails an immense social stigma in various societies [2,3]. Table 1 portrays the statistics of India and world affected with HIV in contemporary years. By

the early 1990's, the first antiviral drugs were developed to suppress HIV. Although AIDS cannot be cured completely, there are medications that can be used to prevent the arrival of the condition so that you are able to preserve your health for an extended period of time [4]. These medications are known as antiretroviral drugs. Currently, there are eight FDA-approved nucleoside/nucleotide reverse transcriptase inhibitors (NRTIs) *viz.*, abacavir, didanosine, emtricitabine, lamivudine, stavudine, zalcitabine, zidovudine, and tenofovir disoprovil fumarate [5] (Fig. 1).

On the other hand, environmental issue is another major issue in both developed and developing countries. Green chemistry is a branch of chemistry that can tackle the environment issues. It emphasizes on conducting synthetic procedures in accordance with its classic 12 principles [6], *viz.*, promoting the sustainability of chemical procedures, energy efficiency, lessening the carcinogenicity of reagents and final

E-mail address: ravichem@kud.ac.in (R.R. Kamble).

^{*} Corresponding author.

Table 1
Statistics of India and world affected with HIV.

HIV statistics	India	World
People with HIV	2.4 million	38.4 million
Adult HIV prevalence	0.20 %	0.22 %
New HIV infections	63,000	1.5 million
Aids-related deaths	42,000	650,000

products, significantly lowering the destruction of the environment and human health, use of smart catalysts, preventing pollution by real-time analysis and use of renewable feed stocks [7,8]. Interestingly, novel molecules as well as well-known chemical compounds can be synthesized using greener approaches.

Green technologies have become prevalent in pharmaceuticals, chemical engineering, and medicinal chemistry, especially when it comes to drug delivery and the fight against tropical and other diseases. Considerable number of green synthesis descriptions also involve biocatalysts or biosynthesis to be revolutionary. Usage of plant extracts [9, 10], fungi, algae or microbes for biosynthesis of compounds and materials are stipulated in order to minimize the effect of hazardous chemicals. The biological approaches are having the advantages of not requiring hazardous chemicals and pollutants, low cost, biocompatibility, pure compound, high yields, no by-products and a large number of precursors (microorganisms and plants). Therefore, biological protocols befit the green chemistry perfectly [11]. Islatravir, (Fig. 2) an inhibitor of HIV, was made entirely using biocatalysis [12].

Biocatalytic cells constitute a prolific natural source for several enzymes which serve as indisputable biocatalysts to catalyze an assortment of biotransformation involving both natural and synthetic targets [13, 14]. Major advancement has been accomplished in achieving an extensive biocatalytic synthesis of nucleoside analogue medicines. The

synthetic pathways for didanosine, molnupiravir, and islatravir (current clinical trials) are almost completely biocatalytic [12]. Biocatalysts can perform magnificently at or close to ambient pressure and temperature. In contrast to manufacturing techniques based upon chemistry, procedures facilitated by biocatalysts can manufacture products of superior value [15,16]. They are environmentally sound and are decomposable at any phase. One such biocatalyst is Baker's yeast.

Baker's yeast can be defined as a eukaryotic single-celled microorganism. It is the generic name for the *Saccharomyces cerevisiae* strain of yeast [17]. It is a renowned biocatalyst that catalyses numerous one-step chemical reactions, *viz.*, reduction of β -keto esters to optically active β -hydroxy esters [18], and for the carbonyl group reduction under mild conditions, with specificities and devoid of byproducts including many other molecules including xanthenes [19–23]. Xanthene has been designated as the oxygen containing heterocyclic ring featuring an exceptionally diverse range of applications [24]. When it comes to the synthesis of this class of chemicals, 1,8-dioxo-octahydroxanthenes remain a significant class of oxygen heterocycles that are of considerable interest due to a spike in the number of their applications both in the field of medicinal chemistry and material science [25,26]. Here we

Fig. 2. Structure of Islatravir, an inhibitor of HIV.

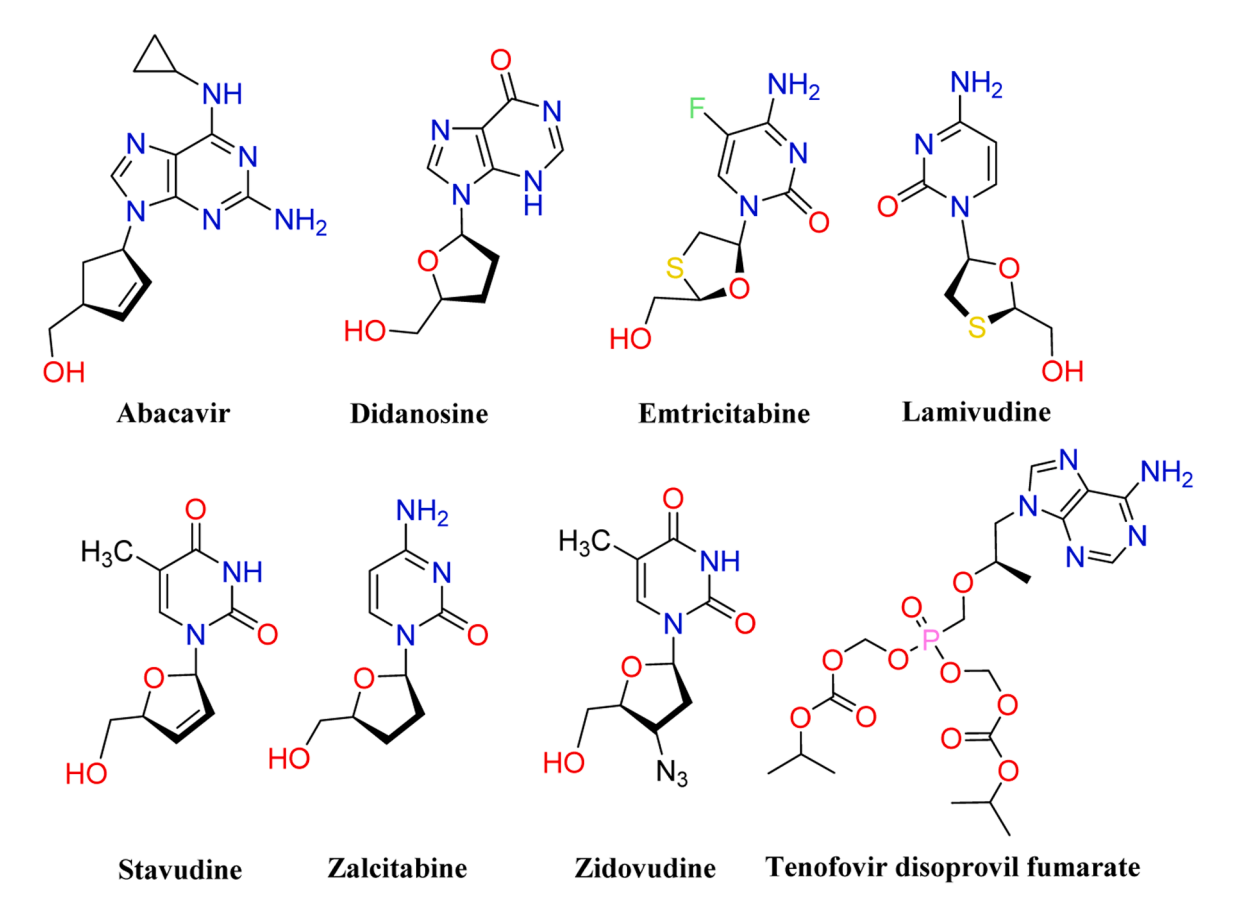


Fig. 1. Some of the FDA-approved antiretroviral drugs for HIV-1 reverse transcriptase.

 Table 2

 Optimization for the synthesis of 1,8-dioxo-octahydroxanthenes 3b-k.

Entry	Solvent	Catalyst (wt. in mg)	Time (min)	Temp °C	Yield (%)
1	EtOH	5	60	RT	20
2	EtOH	5	60	70–80 °C	18
3	MeOH	5	60	RT	5
4	MeOH	5	60	70–80 °C	10
5	MeOH/H ₂ O (1:1)	5	60	RT	20
6	MeOH/H ₂ O (1:1)	5	60	70–80 °C	15
7	EtOH/H ₂ O (1:1)	5	60	RT	30
8	EtOH/H ₂ O (1:1)	5	60	70–80 °C	32
9	THF/H ₂ O (1:1)	5	60	RT	25
10	THF/H ₂ O (1:1)	5	60	70–80 °C	30
11	H_2O	5	60	RT	98

report an assessment of dry Baker's yeast's catalytic activity as green, sustainable, biodegradable, and recyclable heterogeneous catalysts for the formation of 1,8-dioxooctahydroxanthenes *via* water based reaction between aromatic aldehydes and dimedone. Ultimately, our research signifies that 1,8-dioxo-octahydroxanthenes that are proposed here could potentially have HIV inhibiting values, and the fundamental structure of this class of heterocycles might serve as a desirable template for the exploration of novel and prospective HIV drugs. As far as we are aware of the synthesis of xanthenes and considering the foregoing, we infer that this is the first report on a RT stirring enabled biosynthesis of 1,8-dioxooctahydroxanthenes employing the environmentally friendly baker's yeast (*Saccharomyces cerevisiae*) as a whole-cell biocatalyst and their anti-HIV properties [27].

2. Experimental

Unless otherwise noted, all commencing reagents were of analytical grade obtained from different commercial merchants (Sigma-Aldrich, Spectrochem, and Merck companies) and used as provided without further refinement. Melting points were determined on Coslab scientific melting point apparatus. All reactions were tracked by TLC on silica gelprotected aluminum sheets (type 60 F254, Merck) under UV light. The IR spectra were recorded on Nicolet 170 SX FT-IR spectrometer (in cm $^{-1}$ using KBr disc). NMR spectra were documented on Jeol advance NMR spectrometer (400 MHz) in CDCl₃ or DMSO- d_6 as solvent, using TMS as standard (chemical shifts in ppm, units). The mass spectra were carried out using Agilent GC 7820A. Heraeus Carlo Erba 1180 CHN analyzer was used for elemental analyses (C, H, and N). The crystal studies were made using Bruker SMART CCD area-detector diffractometer with monochromatic Mo $K\alpha$ radiation at room temperature.

2.1. General procedure for synthesis of 1,8-dioxo-octahydroxanthenes 3b-k from Baker's yeast

2.1.1. Activation of Baker's yeast

Commercially accessible Baker's dried yeast was utilized entirely for this work. In a beaker (25 ml), warm water (10 ml) of about 35–40 $^{\circ}$ C was taken, and dried yeast (5.0 mg) was deposited in it for 5–10 min. The supernatant liquid was discarded off and the wet yeast was held in reserve. The biocatalyst is now activated and can be used henceforth for the reactions [28].

2.1.2. Reaction protocol

In a RB flask (100 ml), 2 equivalents of 5,5-dimethyl-1,3-cyclohexanedione (1a) and 1 equivalent of aromatic aldehyde (2b-k) were taken along with distilled water (15 ml). To this, activated baker's yeast (5.0 mg) was added. The reaction mixture was kept for RT stirring for 1 h. The completion of the reaction was monitored by TLC using hexane: ethyl acetate (7:3). The reaction mixture was ice quenched and white precipitate was formed. This precipitate obtained was filtered and rinsed with hot water to remove any traces of the catalyst. The resulting product was then purified by recrystallization in ethyl acetate to obtain colourless crystals and the recovered Baker's yeast was reused for 1–3 consecutive runs in this reaction without any considerable loss in the yield and its catalytic activity.

2.1.3. Characterization data

2.1.3.1. 3,3,6,6-tetramethyl-9-phenyl-3,4,5,6,7,9-hexahydro-1H-xanthene-1,8(2H)-dione(3b). Yield: 95 %; white solid; m.p.: 204–206 °C; IR (KBr, cm $^{-1}$): 1581 (xanthene, 2 × C=O); $^1{\rm H}$ NMR (400 MHz, CDCl₃, δ ppm): 1.09 (s, 6H, 2 × CH₃), 1.16 (s, 6H, 2 × CH₃), 2.32–2.34 (d, 4H, 2 × CH₂), 2.38–2.43 (d, 4H, 2 × CH₂), 5.53 (s, 1H, CH), 7.09–7.17 (t, 1H, Ar), 7.23–7.24 (t, 2H, Ar), 7.25–7.27 (d, 2H, Ar). $^{13}{\rm C}$ NMR (100 MHz, CDCl₃, δ ppm): 27.47, 29.76, 31.50, 32.82, 46.51, 47.12, 115.67, 125.93, 126.85, 128.30, 138.13, 155.23, 190.58; GC–MS m/z Calcd Mass: 350; Found: 350 [M $^+$]. CHN analysis for C₂₃H₂₆O₃ Calcd: C, 78.83; H, 7.48; Found: C, 78.81; H, 7.49.

2.1.3.2. 9-(4-bromophenyl)-3,3,6,6-tetramethyl-3,4,5,6,7,9-hexahydro-1H-xanthene-1,8(2H)-dione (3c). Yield: 91 %; white solid; m.p.: 241–243 °C; IR (KBr, cm $^{-1}$): 1581 (xanthene, 2 × C=O); 1 H NMR (400 MHz, CDCl₃, δ ppm): 1.08 (s, 6H, 2 × CH₃), 1.20 (s, 6H, 2 × CH₃), 2.31–2.36 (d, 4H, 2 × CH₂), 2.38–2.42 (d, 4H, 2 × CH₂), 5.43 (s, 1H, CH), 6.93–6.95 (d, 2H, Ar), 7.35–7.37 (d, 2H, Ar). 13 C NMR (100 MHz, CDCl₃, δ ppm): 27.50, 29.10, 32.31, 39.42, 51.47, 113.95, 120.13, 131.24, 131.91, 143.41, 155.09, 198.20. GC–MS m/z Calcd Mass: 428; Found: 428 [M $^{+}$], 430 [M+2]. CHN analysis for C₂₃H₂₅BrO₃ Calcd: C, 64.34; H, 5.87; Found: C, 64.32; H, 5.89.

2.1.3.3. 9-(4-chlorophenyl)-3,3,6,6-tetramethyl-3,4,5,6,7,9-hexahydro-1H-xanthene-1,8(2H)-dione (3d). Yield: 94 %; colourless crystal; m.p.: 232–234 °C; IR (KBr, cm $^{-1}$): 1576 (xanthene, 2 × C=O); 1 H NMR (400 MHz, CDCl₃, δ ppm): 1.08 (s, 6H, 2 × CH₃), 1.20 (s, 6H, 2 × CH₃),

 $\textbf{Scheme 1. Schematic representation for the synthesis of 1,8-dioxo-octahydroxanthenes (\textbf{3b-k}) and substrate scope.}$

Table 3Comparison of the efficacies of a few noteworthy catalysts used during the synthesis of 1,8-dioxo-octahydroxanthenes.

Entry	Catalyst	Catalyst loading	Method	Time (min)	Yield (%)	Ref
1	β-Cyclodextrin	10 mol.%	Reflux (60 °C)	30	91	[26]
2	Wang-OSO ₃ H	10 % w/w	Ultrasonication	60	96	[33]
3	FeNP@SBA-15	0.50 mol.%	Reflux (80 °C)	30	97	[35]
4	CoNP@SBA-15	0.10 mol.%	Reflux (60 °C)	60	98	[31]
5	$(NH_4)_2[Ce(NO_3)_6]$	5 mol.%	Ultrasonication	35	98	[29]
6	Molecular Iodine	0.20 mmol	Reflux (80 °C)	18	90	[34]
5	Baker's Yeast	5 mg	RT	60	98	This work

2.31–2.36 (d, 4H, 2 × CH₂), 2.38–2.42 (d, 4H, 2 × CH₂), 5.45 (s, 1H, CH), 6.98–7.00 (d, 2H, Ar), 7.22–7.24 (d, 2H, Ar). 13 C NMR (100 MHz, CDCl₃, δ ppm): 27.32, 29.28, 32.50, 39.26, 51.00, 112.37, 120.00, 130.67, 131.13, 142.48, 155.58, 190.39. GC–MS m/z Calcd Mass: 384; Found: 384 [M⁺], 386 [M+2]. CHN analysis for $C_{23}H_{25}$ ClO₃ Calcd: C,

71.77; H, 6.55; Found: C, 71.79; H, 6.51.

2.1.3.4. 9-(4-hydroxyphenyl)-3,3,6,6-tetramethyl-3,4,5,6,7,9-hexahydro-1H-xanthene-1,8(2H)-dione (3e). Yield: 96 %; white solid; m.p.: 245–247 °C; IR (KBr, cm $^{-1}$): 1581 (xanthene, 2 × C=O), 3418 (O—H);

Scheme 2. Plausible mechanism for the formation of title compounds 3b-k.

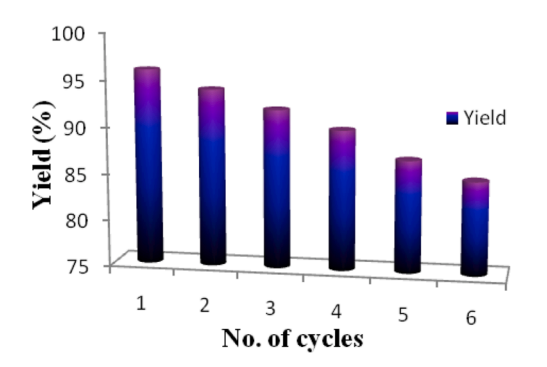


Fig. 3. Catalyst recyclability.

 1 H NMR (400 MHz, CDCl₃, δ ppm): 1.08 (s, 6H, 2 × CH₃), 1.20 (s, 6H, 2 × CH₃), 2.32–2.33 (d, 4H, 2 × CH₂), 2.37–2.41 (d, 4H, 2 × CH₂), 5.45 (s, 1H, CH), 6.11 (s, 1H, OH), 6.67–6.69 (d, 2H, Ar), 6.90–6.92 (d, 2H, Ar). 13 C NMR (100 MHz, CDCl₃, δ ppm): 27.45, 29.71, 31.51, 32.09, 46.50,

47.10, 115.36, 115.88, 127.99, 129.61, 153.88, 157.59, 190.85. GC–MS m/z Calcd Mass: 366; Found: 366 [M $^+$]. CHN analysis for $C_{23}H_{26}O_4$ Calcd: C, 75.38; H, 7.15; Found: C, 75.35; H, 7.19.

2.1.3.5. 3,3,6,6-tetramethyl-9-(4-nitrophenyl)-3,4,5,6,7,9-hexahydro-1H-xanthene-1,8(2H)-dione (3f). Yield: 88 %; pearl white solid; m.p.: 220–222 °C; IR (KBr, cm $^{-1}$): 1579 (xanthene, 2 × C=O); $^1\mathrm{H}$ NMR (400 MHz, CDCl $_3$, δ ppm): 1.10 (s, 6H, 2 × CH $_3$), 1.22 (s, 6H, 2 × CH $_3$), 2.34–2.38 (d, 4H, 2 × CH $_2$), 2.41–2.45 (d, 4H, 2 × CH $_2$), 5.53 (s, 1H, CH), 7.22–7.24 (d, 2H, Ar), 8.11–8.13 (d, 2H, Ar). $^{13}\mathrm{C}$ NMR (100 MHz, CDCl $_3$, δ ppm): 27.34, 29.93, 32.14, 38.79, 39.24, 51.11, 113.89, 123.45, 126.58, 144.62, 151.83, 155.26, 190.56. GC–MS m/z Calcd Mass: 395; Found: 395 [M $^+$]. CHN analysis for C $_{23}\mathrm{H}_{25}\mathrm{NO}_5$ Calcd: C, 69.86; H, 6.37; N, 3.54; Found: C, 69.85; H, 6.33; N, 3.56.

2.1.3.6. 3,3,6,6-tetramethyl-9-(p-tolyl)-3,4,5,6,7,9-hexahydro-1H-xan-thene-1,8(2H)-dione (**3g**). Yield: 90 %; white solid; m.p.: 216–218 °C; IR (KBr, cm $^{-1}$): 1581 (xanthene, 2 × C=O); $^{1}\mathrm{H}$ NMR (400 MHz, CDCl₃, δ ppm): 1.08 (s, 6H, 2 × CH₃), 1.21 (s, 6H, 2 × CH₃), 2.28 (s, 3H, CH₃),

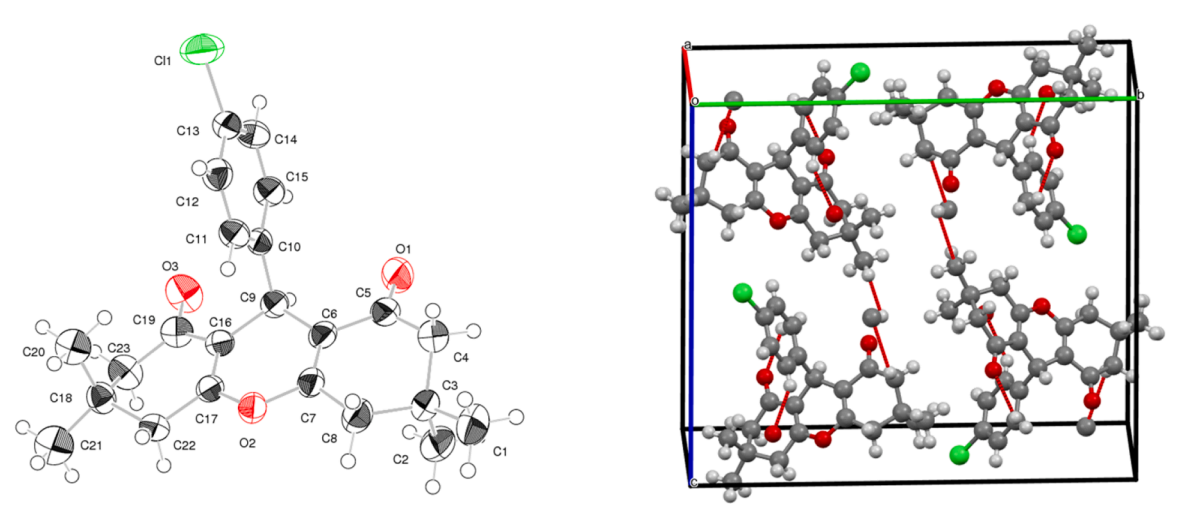


Fig. 4. ORTEP projection and packing diagram of compound 3d.

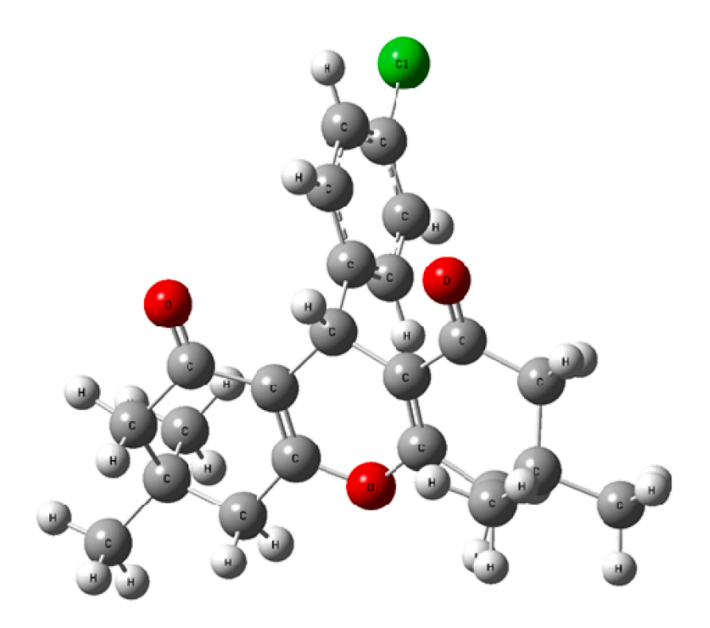


Fig. 5. Optimized structure of the compound 3d.

2.31–2.36 (d, 4H, 2 × CH₂), 2.38–2.42 (d, 4H, 2 × CH₂), 5.49 (s, 1H, CH), 6.95–6.97 (d, 2H, Ar), 7.05–7.07 (d, 2H, Ar). $^{13}\mathrm{C}$ NMR (100 MHz, CDCl₃, δ ppm): 21.47, 27.44, 29.77, 32.10, 39.79, 52.90, 113.74, 127.69, 129.89, 136.06, 141.42, 155.65, 190.75. GC–MS m/z Calcd Mass: 364; Found: 364 [M $^+$]. CHN analysis for C₂₄H₂₈O₃ Calcd: C, 79.09; H, 7.74; Found: C, 79.10; H, 7.77.

2.1.3.7. 9-(4-methoxyphenyl)-3,3,6,6-tetramethyl-3,4,5,6,7,9-hexahydro-1H-xanthene-1,8(2H)-dione (3h). Yield: 94 %; white solid; m.p.: 243–245 °C; IR (KBr, cm $^{-1}$): 1583 (xanthene, 2 × C=O), 2958 (C—H); 1 H NMR (400 MHz, CDCl₃, δ ppm): 1.08 (s, 6H, 2 × CH₃), 1.21 (s, 6H, 2 × CH₃), 2.31–2.36 (d, 4H, 2 × CH₂), 2.37–2.41 (d, 4H, 2 × CH₂), 3.75 (s, 3H, OCH₃), 5.47 (s, 1H, CH), 6.78–6.80 (d, 2H, Ar), 6.97–6.99 (d, 2H, Ar). 13 C NMR (100 MHz, CDCl₃, δ ppm): 27.44, 29.77, 31.47, 32.10, 46.51, 47.14, 55.29, 113.72, 115.87, 127.88, 129.89, 155.19, 157.66, 190.50. GC–MS m/z Calcd Mass: 380; Found: 380 [M $^{+}$]. CHN analysis for C₂₄H₂₈O₄ Calcd: C, 75.76; H, 7.42; Found: C, 75.77; H, 7.43.

2.1.3.8. 9-(4-fluorophenyl)-3,3,6,6-tetramethyl-3,4,5,6,7,9-hexahydro-1H-xanthene-1,8(2H)-dione (3i). Yield: 87 %; white solid; m.p.: 235–237 °C; IR (KBr, cm $^{-1}$): 1581 (xanthene, 2 × C=O); ¹H NMR (400 MHz, CDCl₃, δ ppm): 1.08 (s, 6H, 2 × CH₃), 1.20 (s, 6H, 2 × CH₃), 2.32–2.36 (d, 4H, 2 × CH₂), 2.38–2.42 (d, 4H, 2 × CH₂), 5.46 (s, 1H, CH), 6.91–6.95 (t, 2H, Ar), 7.00–7.04 (t, 2H, Ar). ¹³C NMR (100 MHz, CDCl₃, δ ppm): 27.50, 29.68, 32.82, 39.88, 40.17, 51.77, 114.30, 115.93, 132.79, 141.37, 155.39, 160.60, 190.99. GC–MS m/z Calcd Mass: 368; Found: 368 [M $^{+}$]. CHN analysis for C₂₃H₂₅FO₃ Calcd: C, 74.98; H, 6.84; Found: C, 74.95; H, 6.86.

2.1.3.9. 9-(3-ethoxy-4-hydroxyphenyl)-3,3,6,6-tetramethyl-3,4,5,6,7,9-hexahydro-1H-xanthene-1,8(2H)-dione (3j). Yield: 90 %; white solid; m. p.: 223–225 °C; IR (KBr, cm $^{-1}$): 1589 (xanthene, 2 × C=O) 3523 (O—H); $^1\mathrm{H}$ NMR (400 MHz, CDCl₃, δ ppm): 1.09 (s, 6H, 2 × CH₃), 1.21 (s, 6H, 2 × CH₃), 1.36–1.39 (t, 3H, CH₃), 2.32–2.34 (d, 4H, 2 × CH₂), 2.38–2.40 (d, 4H, 2 × CH₂), 3.94–4.00 (q, 2H, CH₂), 5.46 (s, 1H, CH), 5.50 (s, 1H, OH), 6.54–6.56 (d, 1H, Ar), 6.58 (s, 1H, Ar), 6.78–6.80 (d,

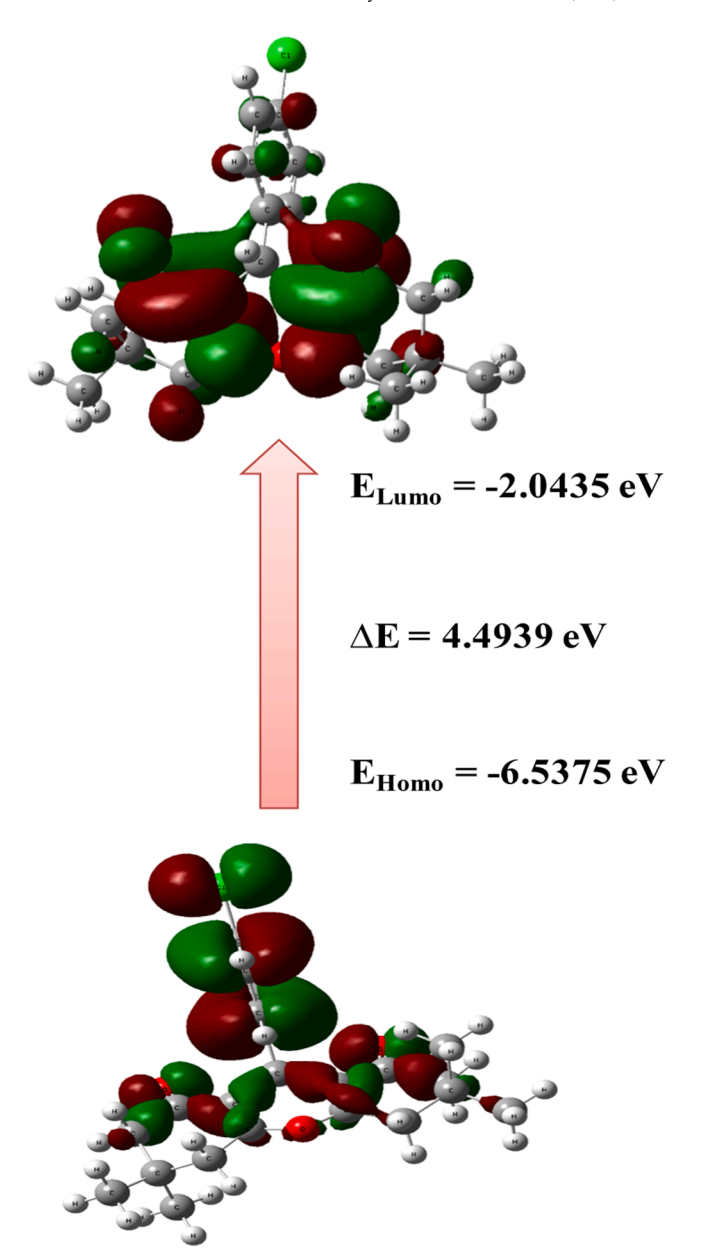


Fig. 6. Frontier molecular orbital of compound3d.

1H, Ar). 13 C NMR (100 MHz, CDCl₃, δ ppm): 14.99, 27.10, 29.94, 31.33, 32.37, 46.46, 47.16, 64.19, 110.74, 114.07, 115.87, 119.49, 129.68, 143.75, 145.51, 155.82, 190.45. GC–MS $\emph{m/z}$ Calcd Mass: 410; Found: 410 [M $^+$]. CHN analysis for $C_{25}H_{30}O_5$ Calcd:, C, 73.15; H, 7.37; Found: C, 73.13; H, 7.33.

2.1.3.10. 9-(4-hydroxy-3-methoxyphenyl)-3,3,6,6-tetramethyl-3,4,5,6,7,9-hexahydro-1H-xanthene-1,8(2H)-dione (3k). Yield: 92 %; white solid; m.p.: 226–228 °C; IR (KBr, cm $^{-1}$): 1575 (xanthene, 2 × C=O), 3430 (O=H); 1 H NMR (400 MHz, CDCl₃, δ ppm): 1.09 (s, 6H, 2 × CH₃), 1.21 (s, 6H, 2 × CH₃), 2.32–2.34 (d, 4H, 2 × CH₂), 2.38–2.41 (d, 4H, 2 × CH₂), 3.74 (s, 3H, CH₃), 5.47 (s, 1H, CH), 5.53 (s, 1H, OH), 6.55–6.57 (d, 1H, Ar), 6.59 (s, 1H, Ar), 6.77–6.79 (d, 1H, Ar). 13 C NMR

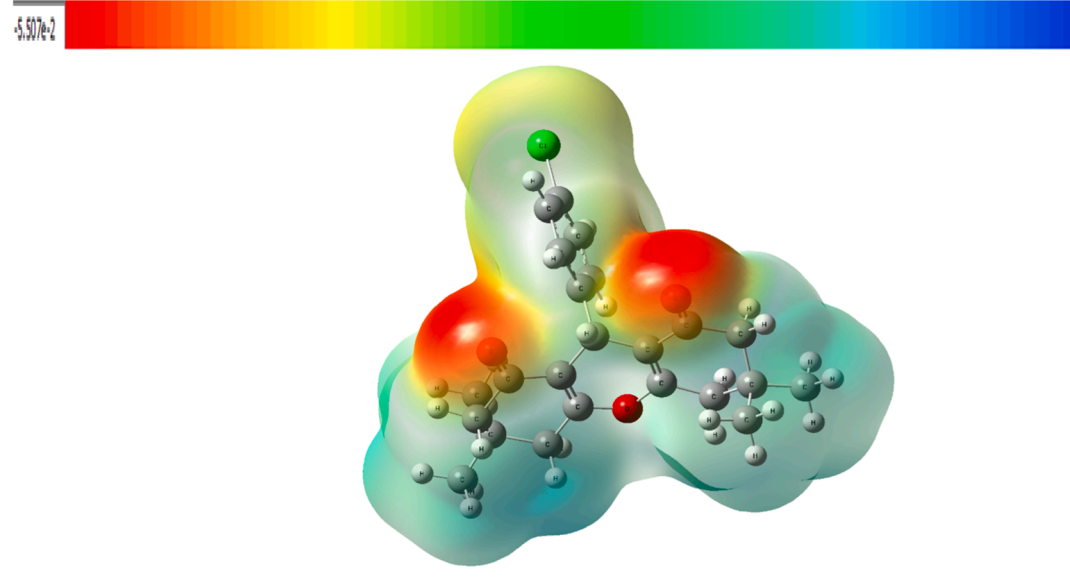


Fig. 7. Molecular electrostatic potential map of compound 3d with colour range $\pm 5.507e^{-2}$.

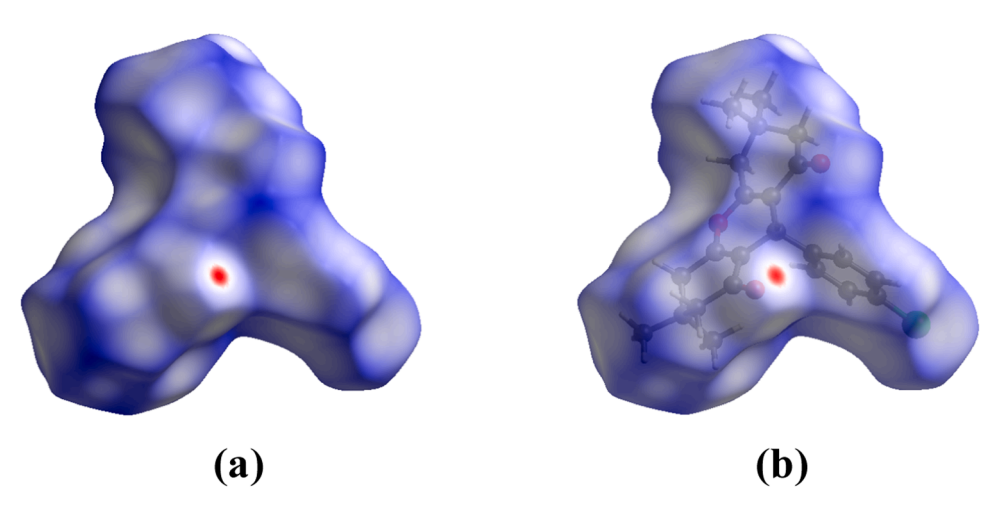


Fig. 8. Hirshfeld surface (a) and Hirshfeld surface transparency (b) for compound C23H25ClO3.

(100 MHz, CDCl₃, δ ppm): 27.16, 29.96, 31.32, 32.39, 46.45, 47.14, 55.72, 109.84, 114.14, 115.86, 119.56, 129.79, 143.64, 146.37, 155.29, 190.50. GC–MS m/z Calcd Mass: 396; Found: 396 [M $^+$]. CHN analysis for $\rm C_{24}H_{28}O_5$ Calcd: C, 72.71; H, 7.12; Found: C, 72.72; H, 7.15.

3. Results and discussion

4. Reaction between dimedone (1a, 2 eq) and aromatic aldehyde (2b-k, 1 eq) was identified as the test reaction in the occurrence of a biocatalyst i.e. Baker's yeast and different reaction parameters were studied for the formation of 1,8-dioxo-octahydroxanthenes (3b-k). Considering the fact that Baker's yeast is activated by water, all the reactions were performed in water at room temperature (RT) under continuous stirring. Despite the fact that reaction conditions were optimized to get the best suited condition for the aforementioned reaction. Initially, Baker's yeast was optimized and the best results were

obtained with 5 mg of the catalyst. To begin, we examined the reactions in various solvents such as ethanol, methanol, water, and mixtures of solvents such as water-ethanol, water-methanol, and water-THF in a 1:1 ratio (Table 2). We however did not get good amount of yield in ethanol and methanol [5-20 % yield] (Table 2, entry 1,3). Even though ethanol is produced by Baker's Yeast, its efficiency may drop down drastically in its concentrated form as it can hinder the activation of the dry yeast in room temperature condition. Therefore, we tried the same solvents at elevated temperature viz., 70-80 °C (Table 2, entry 2, 4), and ended up with moderate yield. Hence, we assessed the identical reaction in diverse solvent systems such as water:ethanol, water:methanol, water:THF in the ratio of 1:1 (Table 2, entry 7, 5, 9). Although the yields rose, they were still insufficient, so we elevated the temperature and found it to be of no much help (Table 2, entry 8, 6, 10). With mere 5 mg of the catalyst we tried the reaction solely with water under RT stirring conditions, and the rate of reaction was spectacularly hastened leading to yields upto 98

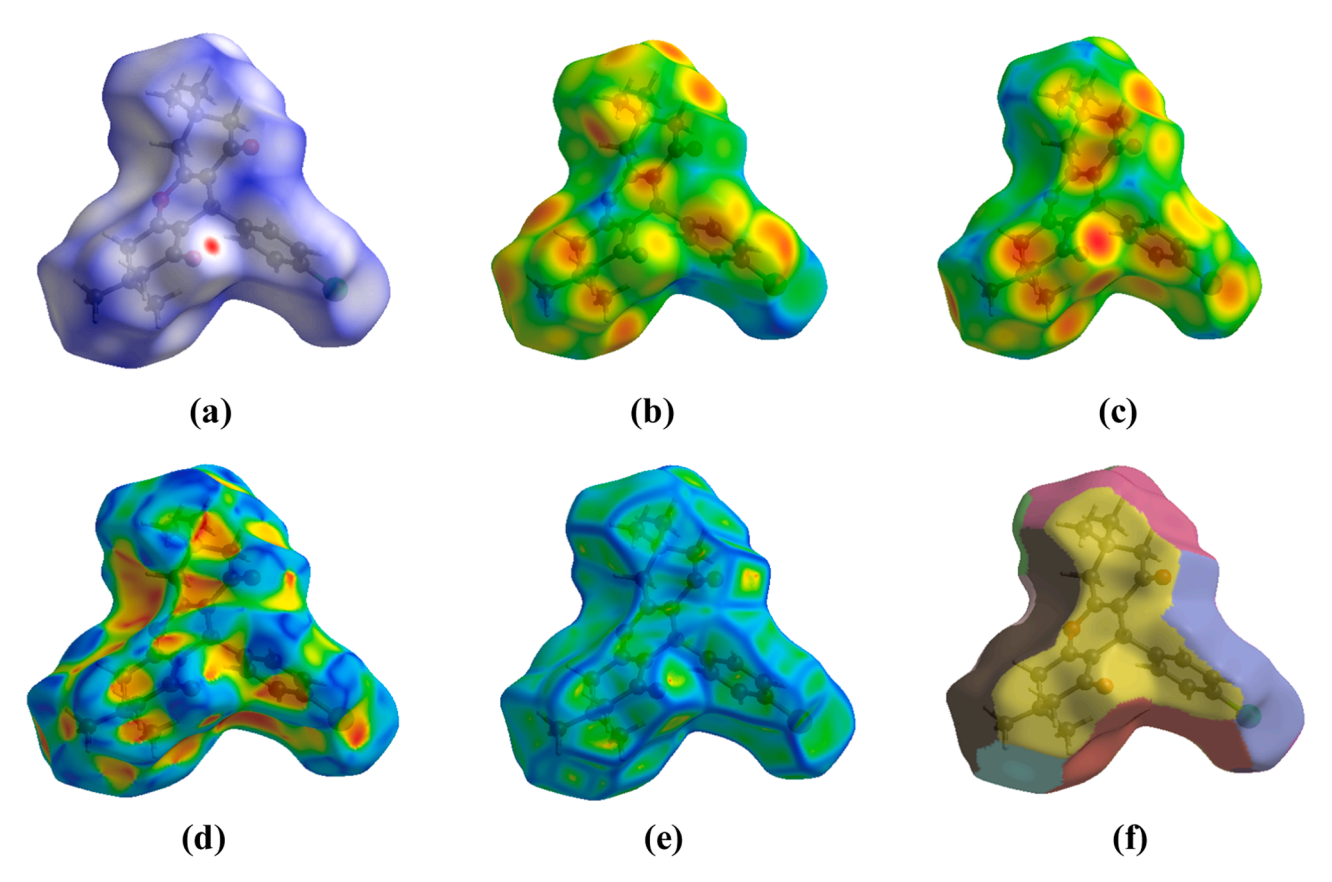


Fig. 9. Hirshfeld surfaces mapped with (a) d_{norm}, (b) d_i, (c) d_e, (d) shape index, (e) curvedness and (f) fragment patch for C₂₃H₂₅ClO₃ compound (3d).

%. It was also found that the efficiency of the catalyst was not influenced by the solvent quantity. Following the aforementioned experimental data, it is quite obvious that water is the most natural and ideal solvent for biocatalysts in terms of viability and activity (Scheme 1).

The synthesis of xanthenes is accelerated by a variety of different catalysts which comprises p-dodecylbenzenesulfonic acid, NaHSO₄-SiO₂, silica sulfuric acid, amberlyst-15, InCl₃/ionic liquid, triethylbenzyl ammonium chloride, ceric ammonium nitrate (CAN), SmCl₃, CoNP@SBA-15, FeNP@SBA-15, Fe₃O₄@SiO₂-SO₃H, Salicylic Acid, Wang resin, HClO₄-SiO₂, ZnO and ZnO-acetyl chloride, solventless Dowex-50 W ion exchange resin protocols, SbCl₃/SiO₂, silica-supported H₁₄[NaP₅W₃₀O₁₁₀] nanoparticles, SiO₂-R-SO₃H, H₃PW₁₂O₄₀ supported MCM-41, DABCO-bromine, cyanuric chloride, trimethylsilylchloride, ZrO(OTf)₂ and [Et₃N-SO₃H]Cl [29-35].

Comparing the dry Baker's yeast with numerous other homogeneous and heterogeneous catalysts believed to have been previously characterized enabled researchers to scrutinize its efficacy and application. The correlation of the findings anticipated for the synthesis of 1,8-dioxo-octahydroxanthenes (3b-k) by means of various conditions revealed that our synthetic approach was advanced to the catalysts previously reported as mentioned in Table 3 in many ways such as, reaction method, reaction time, water as solvent, higher yields, reusability of the catalyst and most importantly non-hazardous to the environment. Employing water as a solvent and obtaining greater yields were the leading deviations observed.

3.1. Plausible mechanism

At this stage baker's yeast is initiated to be executing its function as a biocatalyst as for many of its enzymes it is a whole cell source. The enzymes comprising different amino acid residues are thus readily accessible post yeast disruption, for stimulating reactive functional sites of substrates and reactants [36]. In the preliminary step Baker's Yeast has instigated the condensation of aromatic aldehyde with dimedone to form arylidene dimedone. This is going to evolve into its enol form in the presence of Baker's Yeast. In the second step, the previously formed enol substrate attacks another molecule of dimedone to form an intermediate I. With the elimination of water molecule this intermediate undergoes ring cyclization in the next step. Lastly, with the elimination of another molecule of water, the final product is formed. The plausible mechanism of the formation of 1,8-dioxo-octahydroxanthenes compounds is depicted in Scheme 2.

3.2. Catalyst recycling

In terms of green chemistry, the reusability of the catalyst is crucial [37] and for its development, the capacity of a catalyst to recover and reuse is becoming increasingly important. The catalyst was analyzed under optimal reaction conditions for the condensation and cyclization of dimedone with benzaldehyde as a model reaction. Once the reaction was completed, it was ice quenched, and the product was separated by simple filtration, and it was thoroughly washed with warm water so that there are no traces of the catalyst left behind and the same filtrate was

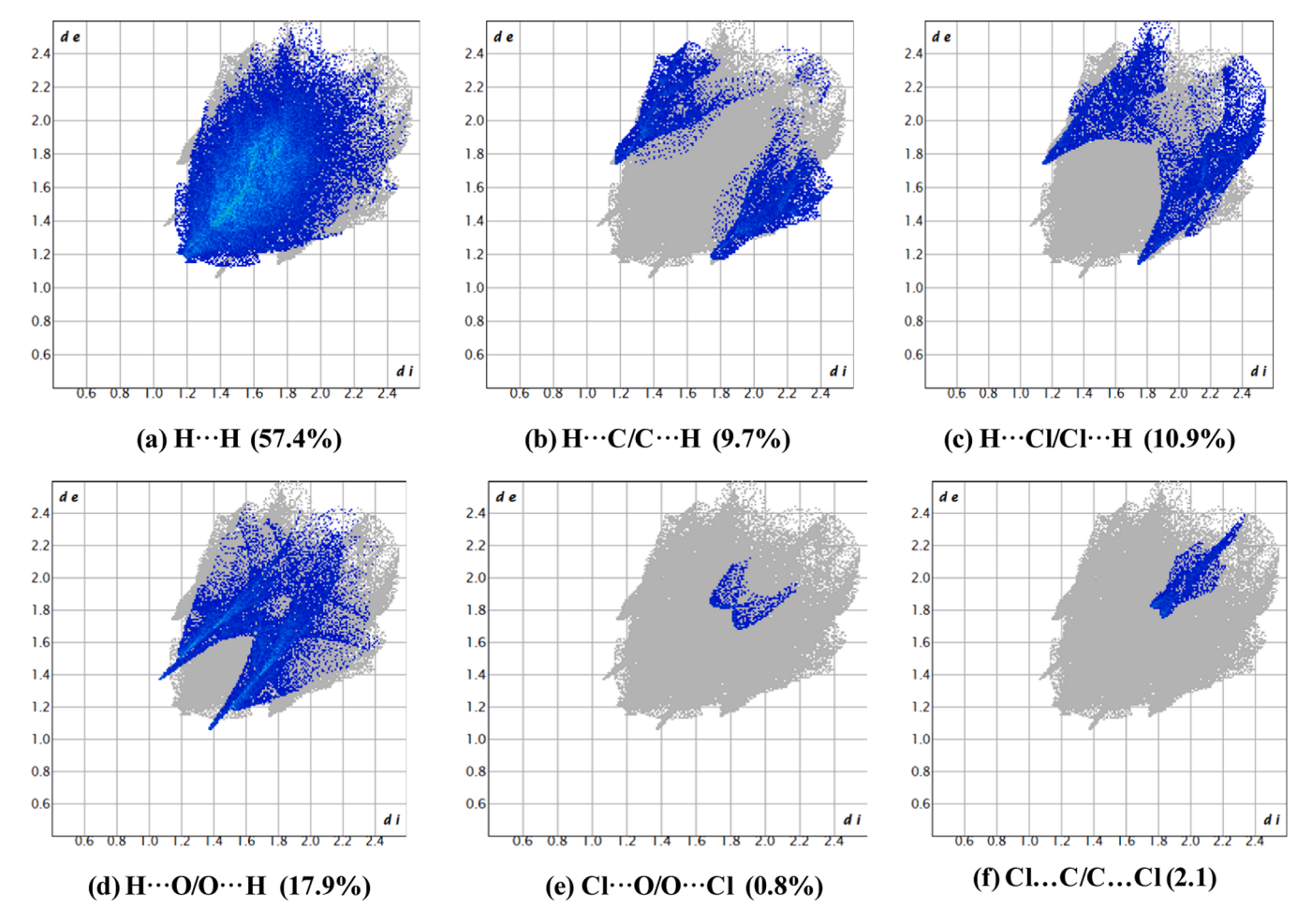


Fig. 10. 2D fingerprint plots for the corresponding H···H, H···C/C···H, H···C/C···H, H···C/C···H, Cl···O/O···Cl and Cl...C/C...Cl interactions.

employed in subsequent cycles to generate compound **3b** under identical reaction conditions. To our astonishment, the catalyst that had been retrieved and reused several times, exhibited no significant loss in its catalytic efficiency as shown in Fig. 3. This is winsome contribution towards the superiority of the current protocol, which has significant benefits including easier reaction setup and product isolation surpassing the available methods for the synthesis of 1,8-dioxo-octahydroxanthenes [38].

3.3. X-ray data, DFT and Hirshfled studies

3.3.1. X-ray data

A single crystal for the compound 3d has been developed by slow evaporation method. The crystalline state of compound 3d, $C_{23}H_{25}O_3Cl$, is determined by long range, accurate 3D instructions and Table S2 in ESI illustrates the detailed x-ray diffraction study report, its crystallographic data and X-ray structure parameters (CCDC No. 2169133). A single molecule forms an asymmetric crystal structure in Fig. 4 and the derivative crystallizes in a monoclinic system in the P 21/n space group. The ORTEP projection of the molecule with thermal ellipsoids drawn at 50 % probability and packing of the molecules are illustrated in Fig. 4.

X-ray crystal structures can also account for unusual electronic or electrostatic properties of a material, shed light on chemical interactions

and processes or serve as the basis for designing pharmaceuticals against diseases. In view of this, X-ray diffraction has been used for identification of well known class of pharmaceutical agents such as β -lactams, tetracycline and Macrolides. Each drugs of this class has a unique XRD pattern that makes their identification easier [39].

The optimized structure of the compound **3d** is illustrated in Fig. 5. Table S3 in ESI data correlates the title compound's optimized geometrical features, like bond lengths and bond angles, with empirically accessible XRD data.

3.3.2. Density function theory (DFT) calculations and frontier molecular orbital (FMO) analysis

DFT is a quantum-mechanical (QM) method used in chemistry and physics to calculate the electronic structure of atoms and molecules including macromolecules. DFT studies have been employed in the medicinal chemistry [40] and also in analyzing the toxicity for pharmaceutical agents acting as anticancer agents or drugs are well documented [41]. Hence, the global reactivity parameters were summarized using HOMO (Highest Occupied Molecular Orbital) and LUMO (Lowest Unoccupied Molecular Orbital) energy values determined by making use of DFT/B3LYP/6–31++ G(d,p) technique [42] and are represented in Table S4 in ESI and plots are depicted in Fig. 6. The 3D-ESP map of compound 3d is depicted in Fig. 7. The Hirshfeld surfaces of the

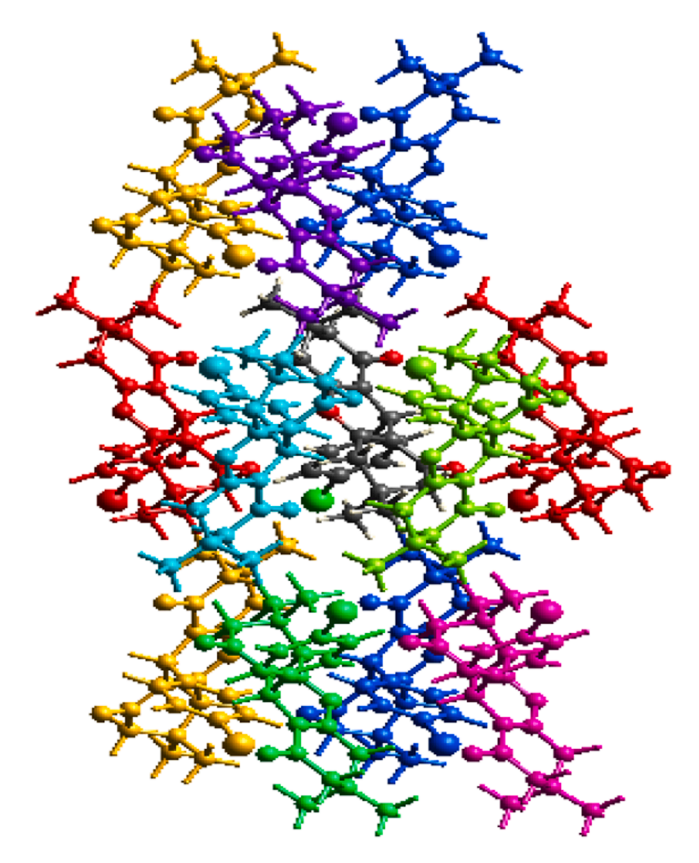


Fig. 11. Molecular pairs involved in the calculation of interaction energies of the $C_{23}H_{25}ClO_3$ compound **3d** along the *c* axis.

compound $C_{23}H_{25}ClO_3$ have indeed been mapped over d_{norm} d_b d_e , shape index, and curvedness in Figs. 8 and 9. And the overall contribution of the various proximities to the total Hirshfeld surface area is depicted in Fig. 10. Fig. 11 depicts the molecules implicated in the computation of the interaction energy of the compound $C_{23}H_{25}ClO_3$ along the c axis. The illustrative representation of coulomb energy, dispersion energy, total energy, and total energy (annotated) of the molecule are represented in Fig. 12.

3.3.3. Molecular electrostatic potential (MEP) analysis

The molecular electrostatic potential (MEP) at a specific point p(x,y,z) in the immediate vicinity of a molecule is the force acting on a positive test charge (a proton) imposed at p through the electrical charge cloud developed through the electrons and nuclei of the molecules. In the domain of biochemistry and pharmacology, molecular electrostatic potentials (MEP's) have been extensively implemented to determine distinctive patterns of positive and negative potentials that either promote or inhibit specific types of biological processes [43]. The primary structural characteristics of $C_{23}H_{25}O_3Cl$ compound that are crucial for its activities will be evaluated via MEP maps (Fig. 7.), and its potential interactions involving a molecular receptor will be investigated by means of recognition in a biological process. In order to synthesize novel molecules we need to elucidate the structure-activity relationship of bioactive compounds, hence, excessive investigation of their potential is desirable in designing biologically active compounds.

3.3.4. Hirshfeld analysis

Hirshfeld surfaces and the associated 2D-fingerprint plots were estimated using CrystalExplorer17 that accepts a structure input file in CIF format from single crystal XRD analysis. Table S5 in ESI provides surface property information of compound $C_{23}H_{25}ClO_3$. Table S6 in ESI provides different interaction energies of molecular pairs in kJ/mol and Table S7 in ESI provides lattice energy calculations of $C_{23}H_{25}ClO_3$ compound in (Å) Lattice energy calculations.

3.4. Molecular docking studies

Molecular docking studies were carried out on the crystal structure of a catalytic complex of HIV-1 reverse transcriptase [44]: implications for nucleoside analogue drug resistance [45] (PDB ID 1RTD, 3.20 Å X-ray Diffraction) using the surflex-dock programme of sybyl-X 2.0 software to analyze the mechanism and detailed intermolecular interactions between the synthesized compounds. As demonstrated in Fig. 13A and B, all inhibitors were docked into the active site of the enzyme. Table 4 illustrates the anticipated binding energies of the substances. The docking analysis indicated that every single drug performed exceptionally well against the enzyme. As illustrated in the Fig. 14 (A-C), compound 3j includes two hydrogen bonding interactions at the active site of the enzyme (PDB ID: 1RTD), among which a bonding interaction is raised from oxygen atom existing in the xanthene ring with hydrogen atom of ARG72 (—O—- H-ARG72, 2.15 Å) and oxygen atom of hydroxyl group existing on the 4th position of phenyl ring tends to make an interaction with hydrogen atom of LYS65 (-O-- H-LYS65, 2.73 Å). According to Fig. 15(A-C), compound 3k does have two hydrogen bonding interactions at the active site of the enzyme (PDB ID: 1RTD), one of which is a bonding interaction raised from an oxygen atom existing in the xanthene ring with a hydrogen atom of LYS65 (-O-H-LYS65, 1.80 Å), and another oxygen atom of the methoxy group, which is situated on the third position of the phenyl ring makes an interaction with the hydrogen atom of ARG72 (-O-H-ARG72, 2.06 Å). The 1RTD ligand displayed eight H-bonding interactions, as shown in Fig. 16(A-C). Fig. 17(A and B) depicts the hydrophobic and hydrophilic amino acids that surround the examined compounds 3i & 3k. Docking studies employing Surflex-Dock confirmed that practically all of the synthesized compounds inhabited the very same binding sites as 1RTD ligand, and also had same sort of interactions with amino acid residues (ARG72 and LYS65) as 1RTD ligand. Every single compound had a consensus score in the range of 6.68-3.05, suggesting a summary of all ligand-enzyme interactions.

4. Conclusions

The HIV/AIDS epidemic has persistently contributed to widespread human diseases and mortality. We have developed Baker's Yeast to be a low-cost, green, biodegradable, and efficient biocatalyst with an ecologically suitable synthetic protocol to explore the synthesis of 1,8-dioxooctahydroxanthenes at room temperature as the inhibitors of HIV reverse transcriptase. This protocol has provided remarkable yields (87 % to 96 %) at short reaction time with minimal catalyst concentration in water in its purest form that afforded crystals and the crystal structure analysis and hydrogen bonding patterns of compound 3d developed using the same methodology, in addition to the DFT and Hirshfeld analysis, have been reported. Most synthesized compounds exhibited high C-Score values, reflecting a favorable binding and subsequently suppression against HIV-1 reverse transcriptase and compound 3j comprising a hydroxy and ethoxy groups exhibiting maximum

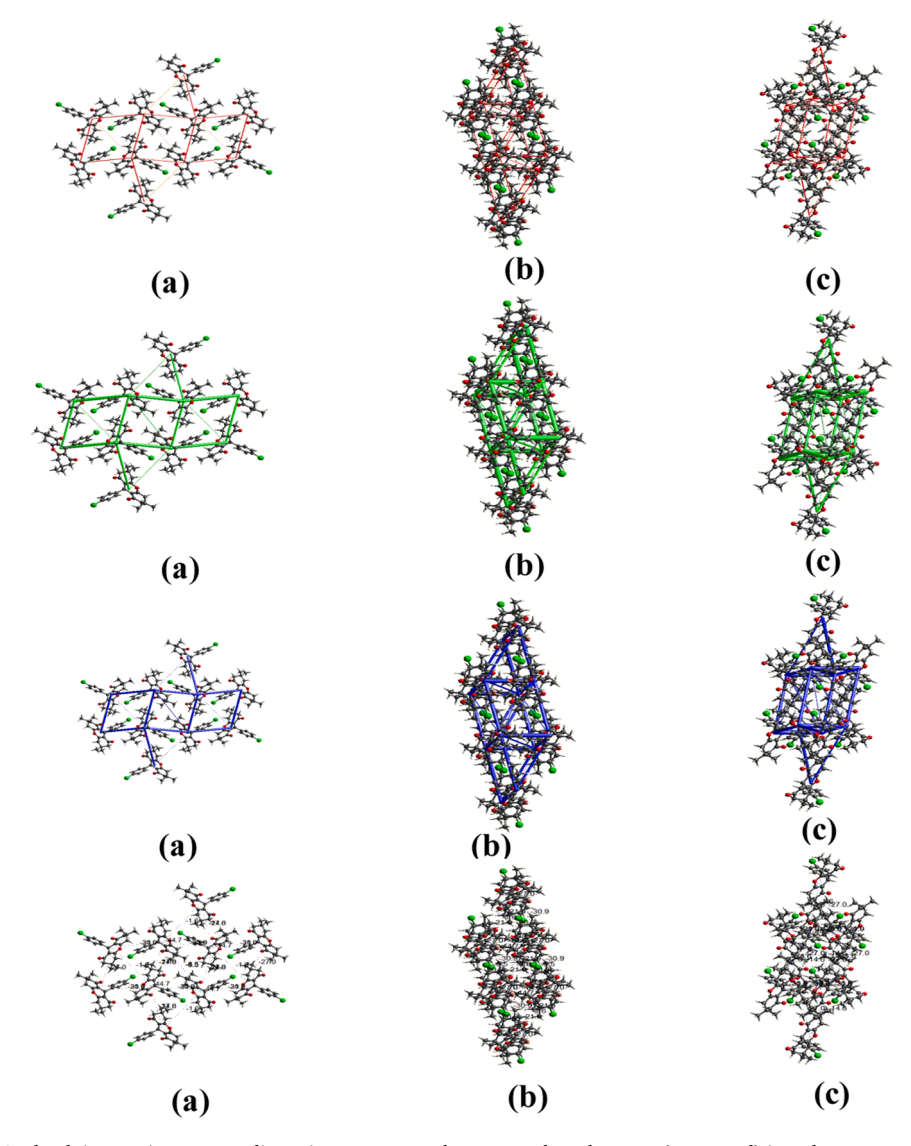


Fig. 12. Illustration of the Coulomb interaction energy, dispersion energy, total energy and total energy (annotated) in red, green, and blue colours along the a, b, and c axes, respectively of compound 3d.

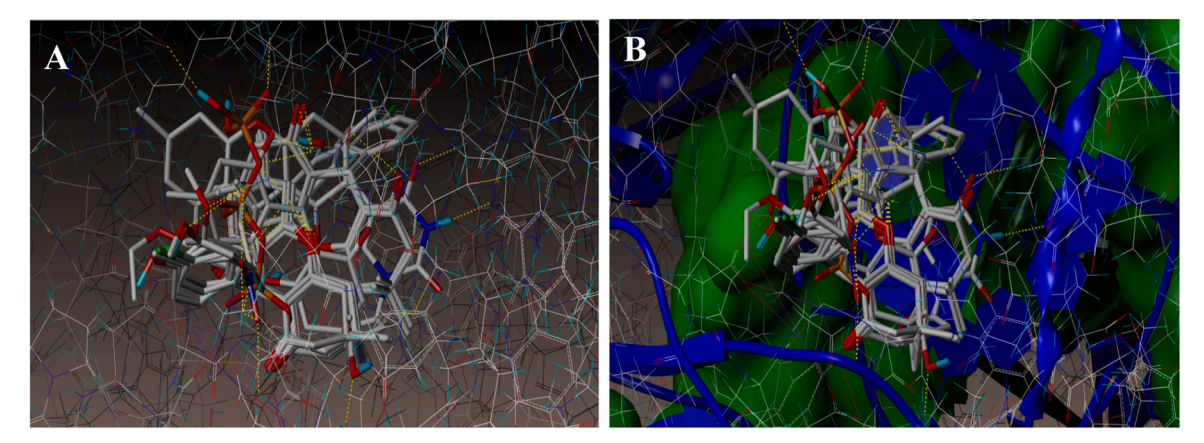


Fig. 13. Docked view of all the compounds at the active site of the enzyme PDB ID: 1RTD.

Table 4Surflex Docking score (kcal/mol) of the derivatives.

Compounds	C score ^a	Crash score ^b	Polar score ^c	D score ^d	PMF score ^e	G score ^f	Chem score ^g
1RTD_ligand	9.25	-1.02	7.55	-164.354	-188.491	-242.801	-28.778
3b	3.83	-2.12	0.06	-115.172	-104.319	-235.298	-17.856
3c	4.73	-4.21	1.93	-101.615	-68.820	-253.217	-28.360
3d	4.41	-4.00	1.75	-102.720	-72.898	-251.318	-27.642
3e	3.05	-2.91	1.09	-79.986	-123.977	-211.681	-22.387
3f	5.79	-1.29	3.91	-91.971	-100.068	-181.110	-25.342
3g	5.90	-4.13	2.21	-103.630	-64.593	-252.634	-28.888
3h	6.34	-3.30	2.07	-86.984	-77.521	-248.598	-27.585
3i	4.12	-1.98	0.16	-112.118	-107.498	-229.927	-17.680
3j	6.68	-3.31	1.81	-85.329	-86.091	-256.489	-27.312
3k	5.98	-4.19	3.23	-84.852	-79.666	-238.180	-30.276

^a CScore (Consensus Score) - This is an integration of the number of popular scoring functions for assessing the affinity of synthesized compounds docked into the active site of the protein and this is the total score.

^g Chem-score - This indicates the H-bonding, lipophilic contact and rotational entropy, along with an intercept term.

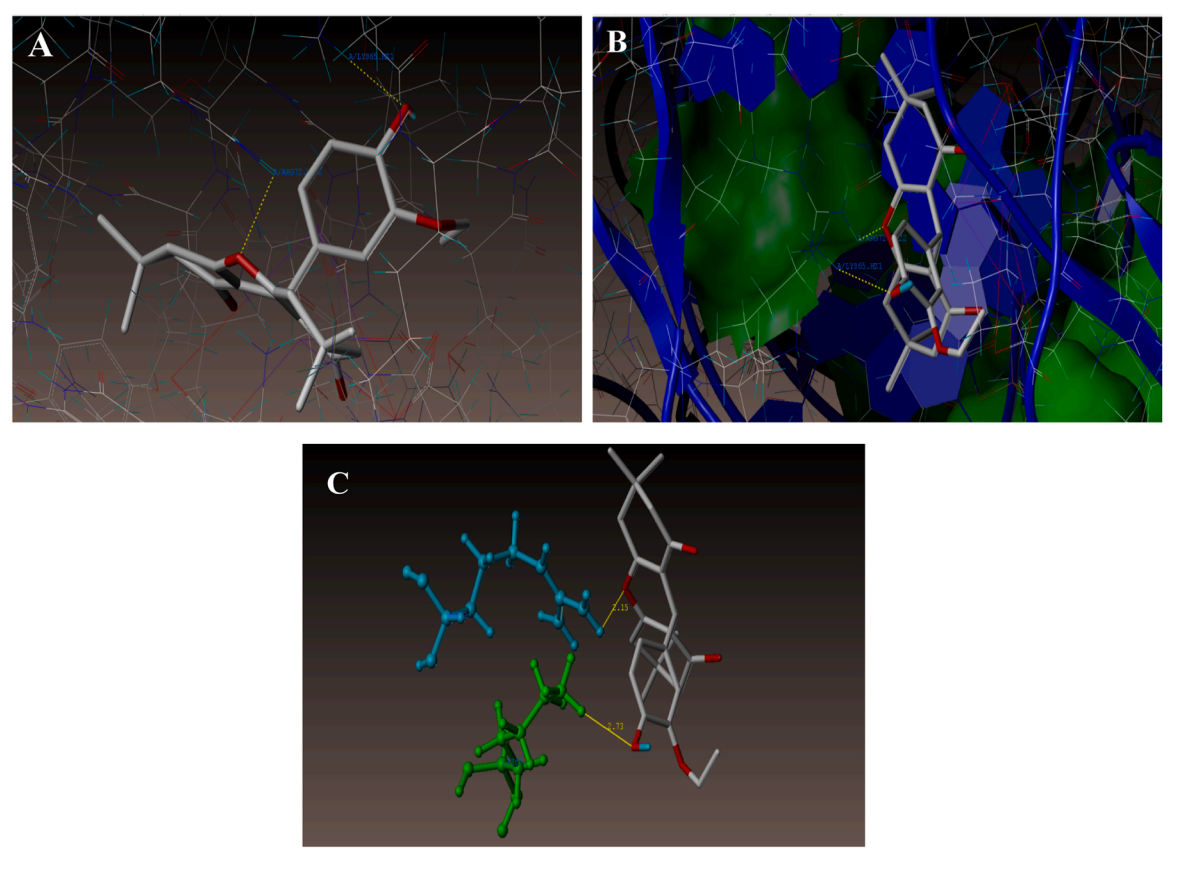


Fig. 14. Interaction of 3j at the binding site of the enzyme (PDB ID: 1RTD).

^b Crash-score - It indicates the unsuitable penetration into the docking pocket. Crash scores nearer to 0 are favorable. The negative numbers illustrate the penetration.

^c Polar Score - The polar score is a measure of polar interactions to the total score and is useful for excluding docking results that make no hydrogen bonds.

^d D-score - It reveals the charge and van der Waals interactions between the receptor and the reported compounds.

^e PMF-score - This indicates the Helmholtz free energies of interactions between the receptor and the atom pairs of the synthesized molecule or the reference compound (Potential of Mean Force, PMF).

f G-score - It is a measure of H-bond between the (compound-protein), and internal (compound-compound).

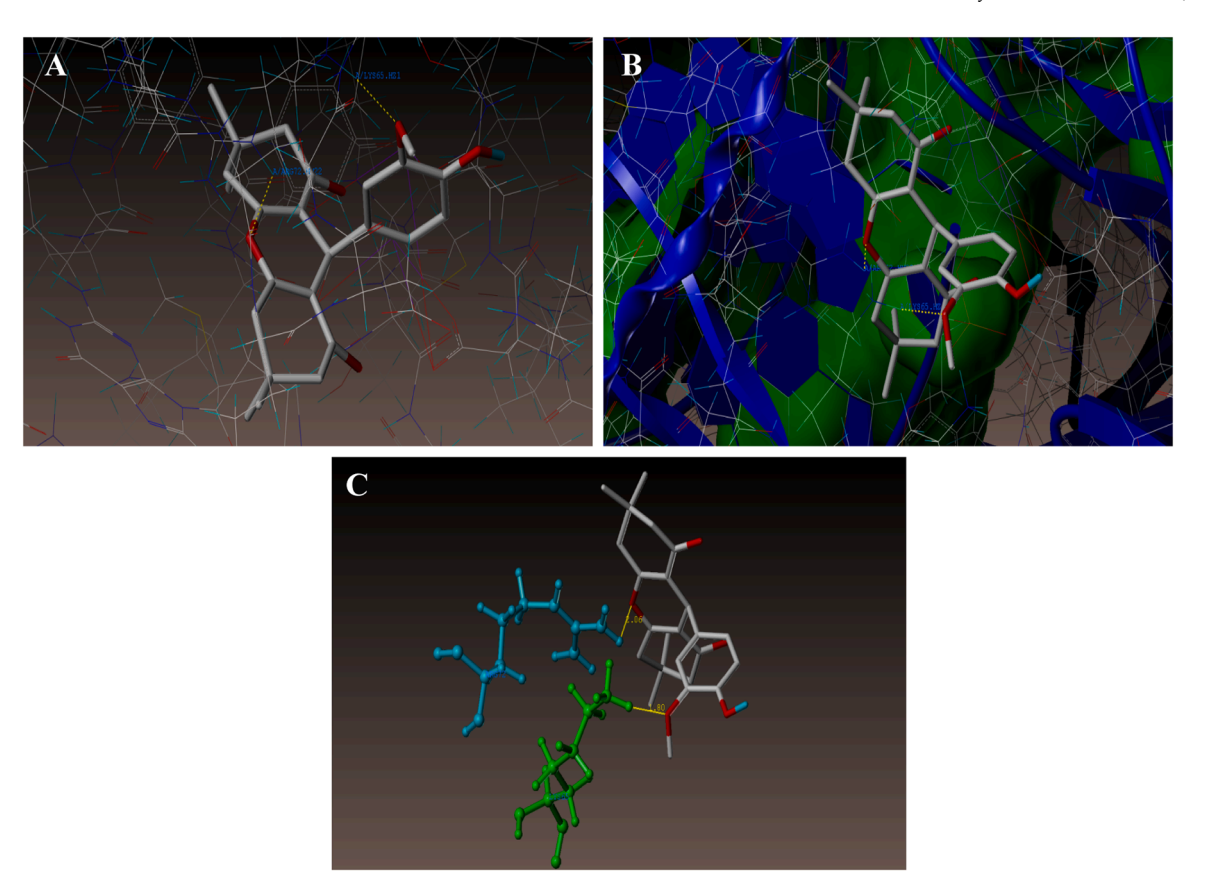
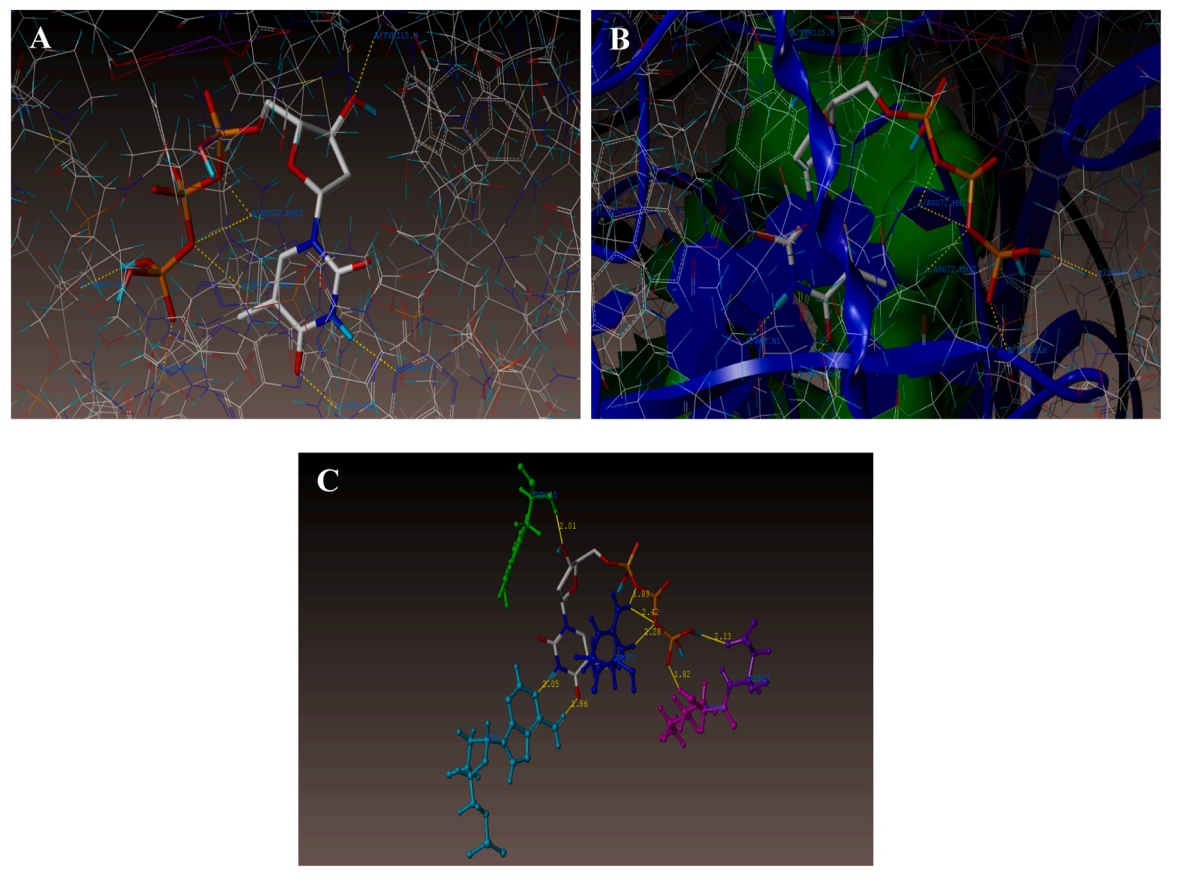


Fig. 15. Interaction of 3k at the binding site of the enzyme (PDB ID: 1RTD).



 $\textbf{Fig. 16.} \ \ \textbf{Interaction of 1RTD_ligand at the binding site of the enzyme (PDB \ ID: 1RTD).}$

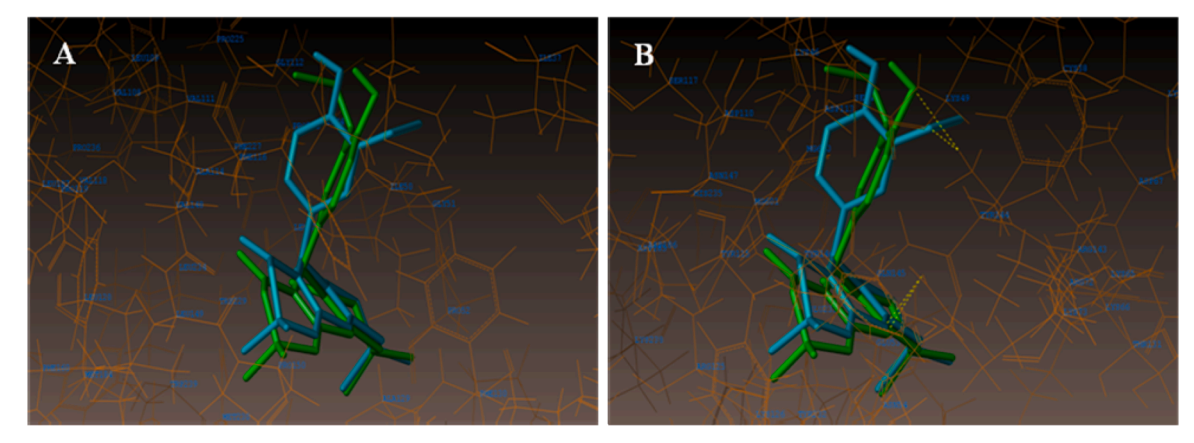


Fig. 17. A) Hydrophobic amino acids surrounded to compounds 3j (green colour) and 3k (cyan colour). B) Hydrophilic amino acids surrounded to compounds 3j and 3k.

C-Score value is considered to be propitious.

CRediT authorship contribution statement

Swati R. Hoolageri: Writing – original draft, Visualization, Validation, Software, Methodology, Investigation, Formal analysis, Conceptualization. Ravindra R. Kamble: Writing – review & editing, Visualization, Validation, Supervision, Resources. Aravind R. Nesaragi: Visualization, Validation, Software, Formal analysis. H.C. Devarajegowda: Validation, Software, Resources. Manojna R. Nayak: Visualization, Formal analysis. Tukaram V. Metre: Visualization, Formal analysis. Shrinivas D. Joshi: Validation, Software, Investigation, Data curation. Roopadevi P: Visualization, Validation, Software, Investigation, Formal analysis, Data curation. Vindu Vahini M: Visualization, Formal analysis.

Declaration of competing interest

The authors declare that they have no known competing financial interests or personal relationships that could have appeared to influence the work reported in this paper.

Data availability

The data that support the findings of this study are available in the supplementary material of this article.

Acknowledgements

The authors are grateful to DST-PURSE Phase-II, SAIF, New Delhi, University Scientific Instrumentation Center (USIC), Karnatak University Dharwad. The authors acknowledge Yuvaraja's College, University Of Mysore, Mysuru, India, for providing the crystal data and CNMS, Jain University, Bangalore for providing the GC–MS data.

Supplementary materials

Supplementary material associated with this article can be found, in the online version, at doi:10.1016/j.molstruc.2024.139290.

References

[1] K. Nandi, P. Bakshi, S. Sarkar, S. Guha, S. Sarkar, M. Sahoo, S. Mandal, T. M. Chatterjee, B. Saha, A. Ghosh, D.J. Sen, S. Das, P.R. Bhattacharya, B. Mahanti, Analysis of the blueprint of HIV, Eur. J. Biomed. Pharm. Sci. 7 (2020) 306–318.

- [2] A. Baghaei Lakeh, N. Ghaffarzadegan, Global trends and regional variations in studies of HIV/AIDS, Sci. Rep. 7 (2017) 1–8, https://doi.org/10.1038/s41598-017-04507
- [3] B. Armoon, M.J. Fleury, A.H. Bayat, Y. Fakhri, P. Higgs, L.F. Moghaddam, L. Gonabadi-Nezhad, HIV related stigma associated with social support, alcohol use disorders, depression, anxiety, and suicidal ideation among people living with HIV: a systematic review and meta-analysis, Int. J. Ment. Health Syst. 16 (2022) 1–17, https://doi.org/10.1186/s13033-022-00527-w.
- [4] A. Kapila, S. Chaudhary, R.B. Sharma, H. Vashist, S.S. Sisodia, A. Gupta, A review on: HIV AIDS, Indian J. Pharm. Biol. Res. 4 (2016) 69–73, https://doi.org/ 10/30750/jinbr.4.3.9
- [5] E.J. Arts, D.J. Hazuda, HIV-1 antiretroviral drug therapy, Cold Spring Harb. Perspect. Biol. 2 (2012) a007161, https://doi.org/10.1101/cshperspect.a007161, 1–23.
- [6] G. Aiswarya, K. Divekar, A review on synthesis of various oxadiazole derivatives applying green chemistry methods, Der Pharm. Lett. 13 (2021) 108–131.
- [7] A.R. Nesaragi, R.R. Kamble, P.K. Bayannavar, S.K.J. Shaikh, S.R. Hoolageri, B. Kodasi, S.D. Joshi, V.M. Kumbar, Microwave assisted regioselective synthesis of quinoline appended triazoles as potent anti-tubercular and antifungal agents via copper (I) catalyzed cycloaddition, Bioorg. Med. Chem. Lett. 41 (2021) 127984, https://doi.org/10.1016/j.bmcl.2021.127984.
- [8] A.R. Nesaragi, R.R. Kamble, S. Dixit, B. Kodasi, S.R. Hoolageri, P.K. Bayannavar, J. P. Dasappa, S. Vootla, S.D. Joshi, V.M. Kumbar, Green synthesis of therapeutically active 1,3,4-oxadiazoles as antioxidants, selective COX-2 inhibitors and their in silico studies, Bioorg. Med. Chem. Lett. 43 (2021) 1–7, https://doi.org/10.1016/j.bmcl.2021.128112.
- [9] S.R. Hoolageri, A.R. Nesaragi, R.R. Kamble, S. Dixit, S. Vootla, S.D. Joshi, S. J. Shaikh, Green synthesis of novel triazolothiadiazine-coumarins catalyzed by agro waste extract: an approach towards in-silico and in-vitro anti-fungal activity, ChemistrySelect 7 (2022) e202200077, https://doi.org/10.1002/slct.202200077.
- [10] A.R. Nesaragi, R.R. Kamble, S.R. Hoolageri, A. Mavazzan, S.F. Madar, A. Anand, S. D. Joshi, WELPSA: a natural catalyst of alkali and alkaline earth metals for the facile synthesis of tetrahydrobenzo[b]pyrans and pyrano[2,3-d]pyrimidinones as inhibitors of SARS-CoV-2, Appl. Organomet. Chem. 36 (2022) 1–21, https://doi.org/10.1002/aoc.6469.
- [11] O.V. Kharissova, B.I. Kharisov, C.M.O. González, Y.P. Méndez, I. López, Greener synthesis of chemical compounds and materials, R. Soc. Open Sci. 6 (2019) 191378, https://doi.org/10.1098/rsos.191378.
- [12] L. Nagy-Györ, M. Lăcătuş, D. Balogh-Weiser, P. Csuka, V. Bódai, B. Erdélyi, Z. Molnár, G. Hornyánszky, C. Paizs, L. Poppe, How to turn yeast cells into a sustainable and switchable biocatalyst? On-demand catalysis of ketone bioreduction or acyloin condensation, ACS Sustain. Chem. Eng. 7 (2019) 19375–19383. https://doi.org/10.1021/acssuschemeng.9b03367.
- [13] C.K. Winkler, J.H. Schrittwieser, W. Kroutil, Power of biocatalysis for organic synthesis, ACS Cent. Sci. 7 (2021) 55–71, https://doi.org/10.1021/ acscentsci.0c01496.
- [14] S.C. Cosgrove, G.J. Miller, Advances in biocatalytic and chemoenzymatic synthesis of nucleoside analogues, Expert Opin. Drug Discov. 17 (2022) 355–364, https://doi.org/10.1080/17460441.2022.2039620.
- [15] R.A. Sheldon, J.M. Woodley, Role of biocatalysis in sustainable chemistry, Chem. Rev. 118 (2018) 801–838, https://doi.org/10.1021/acs.chemrev.7b00203.
- [16] N. Weber, M. Gorwa-Grauslund, M. Carlquist, Engineered baker's yeast as whole-cell biocatalyst for one-pot stereo-selective conversion of amines to alcohols, Microb. Cell Factories 13 (2014) 1–9, https://doi.org/10.1186/s12934-014-0118-z.
- [17] B.M. Sahoo, B.K. Banik, Baker's yeast-based organocatalysis: applications in organic synthesis, Curr. Organocatal. 6 (2018) 158–164, https://doi.org/10.2174/ 2213337206666181211105304.
- [18] J.H. Lee, Synthesis of Hantsch 1,4-dihydropyridines by fermenting bakers' yeast, Tetrahedron Lett. 46 (2005) 7329–7330, https://doi.org/10.1016/j. tetlet.2005.08.137.

- [19] N. Mashal, J. Azizian, K. Larijani, F. Nematollahi, H. Azizian, Baker's yeast promoted one-pot synthesis of new 1,2,4-triazolpyrimido-1,3,4-oxadiazoles: investigation of antioxidant and antimicrobial activity, Polycycl. Aromat. Compd. (2022) 1–18, https://doi.org/10.1080/10406638.2022.2094974.
- [20] A.S. Chavan, A.S. Kharat, M.R. Bhosle, R.A. Mane, A convenient Baker yeast accelerated, one-pot synthesis of pentasubstituted thiopyridines, Synth. Commun. 47 (2017) 1777–1782, https://doi.org/10.1080/00397911.2017.1350982.
- [21] S. Santra, Baker's yeast catalyzed multicomponent reactions: a new hope? ChemistrySelect 4 (2019) 12630–12637, https://doi.org/10.1002/slct.201902263.
- [22] U.R. Pratap, J.R. Mali, D.V. Jawale, R.A. Mane, Bakers' yeast catalyzed synthesis of benzothiazoles in an organic medium, Tetrahedron. Lett. 50 (2009) 1352–1354, https://doi.org/10.1016/j.tetlet.2009.01.032.
- [23] B.S. Londhe, S.L. Khillare, A.M. Nalawade, R.A. Mane, Bakers yeast catalyzed and ultrasound accelerated synthesis of 2-amino-2-chromenes, Int. J. Adv. Res. 9 (2021) 189–195, https://doi.org/10.21474/ijar01/12294.
- [24] M. Maia, D.I.S.P. Resende, F. Dur, M.M.M. Pinto, E. Sousa, Xanthenes in medicinal chemistry-synthetic strategies and biological activities, Eur. J. Med. Chem. 210 (2021) 113085, https://doi.org/10.1016/j.ejmech.2020.113085.
- [25] A. Ilangovan, S. Malayappasamy, S. Muralidharan, S. Maruthamuthu, A highly efficient green synthesis of 1, 8-dioxo-octahydroxanthenes, Chem. Cent. J. 5 (2011) 2–7, https://doi.org/10.1186/1752-153X-5-81.
- [26] A.B. Waghamare, S.S. Deshmukh, G.M. Bondle, A.V. Chate, A highly efficient green synthesis of 1,8-dioxo-octahydroxanthenes using β-Cyclodextrin as an environmentally compatible catalyst, Chem. Biol. Interface 8 (2018) 151–161.
- [27] A.V. Chate, S.B. Sukale, R.S. Ugale, C.H. Gill, Baker's yeast: an efficient, green, and reusable biocatalyst for the one-pot synthesis of biologically important Nsubstituted decahydroacridine-1,8-dione derivatives, Synth. Commun. 47 (2017) 409–420, https://doi.org/10.1080/00397911.2016.1266501.
- [28] A. Mahanta, A. Dutta, A.J. Thakur, U. Bora, Biocatalysis with Baker's yeast: a green and sustainable approach for C–B bond cleavage of aryl/heteroarylboronic acids and boronate esters at room temperature, Sustain. Chem. Pharm. 19 (2021) 100363, https://doi.org/10.1016/j.scp.2020.100363.
- [29] N. Mulakayala, G. Pavan Kumar, D. Rambabu, M. Aeluri, M.V. Basaveswara Rao, M. Pal, A greener synthesis of 1,8-dioxo-octahydroxanthene derivatives under ultrasound, Tetrahedron Lett. 53 (2012) 6923–6926, https://doi.org/10.1016/j. tetlet.2012.10.024.
- [30] F. Nemati, S. Sabaqian, Nano-Fe₃O₄ encapsulated-silica particles bearing sulfonic acid groups as an efficient, eco-friendly and magnetically recoverable catalyst for synthesis of various xanthene derivatives under solvent-free conditions, J. Saudi Chem. Soc. 21 (2017) S383–S393, https://doi.org/10.1016/j.jscs.2014.04.009.
- [31] F. Rajabi, M.P-de Dios, M. Abdollahi, R. Luque, Aqueous synthesis of 1,8-dioxooctahydroxanthenes using supported cobalt nanoparticles as a highly efficient and recyclable nanocatalyst, Catal. Commun. 120 (2019) 95–100, https://doi.org/ 10.1016/j.catcom.2018.10.004.
- [32] F. Mohamadpour, M. Feilizadeh, Salicylic acid as a bio-based and natural bronsted acid catalyst promoted green and solvent-free synthesis of various xanthene derivatives, Chem. Methodol. 4 (2020) 647–659, https://doi.org/10.22034/ chemm 2020 109841
- [33] M. Manikanttha, K. Deepti, M.B. Tej, A.G. Reddy, R. Kapavarapu, M.V.B. Rao, M. Pal, Wang resin catalyzed green synthesis of 1,8-dioxo-octahydroxanthene

- derivatives and their in silico/in vitro evaluation against SIRT1, J. Mol. Struct. 1264 (2022) 133313, https://doi.org/10.1016/j.molstruc.2022.133313.
- [34] N. Mulakayala, P.V.N.S. Murthy, D. Rambabu, M. Aeluri, R. Adepu, G.R. Krishna, C.M. Reddy, K.R.S. Prasad, M. Chaitanya, C.S. Kumar, M.V. Basaveswara Rao, M. Pal, Catalysis by molecular iodine: a rapid synthesis of 1,8-dioxo-octahydrox-anthenes and their evaluation as potential anticancer agents, Bioorg. Med. Chem. 22 (2012) 2186–2191, https://doi.org/10.1016/j.bmcl.2012.01.126.
- [35] F. Rajabi, M. Abdollahi, E.S. Diarjani, M.G. Osmolowsky, O.M. Osmolovskaya, P. Gomez-Lopez, A.R. Puente-Santiago, R. Luque, Solvent-free preparation of 1,8-dioxo-octahydroxanthenes employing iron oxide nanomaterials, Materials 12 (2019) 2386, https://doi.org/10.3390/ma12152386.
- [36] A.S. Chavan, A.S. Kharat, M.R. Bhosle, S.T. Dhumal, R.A. Mane, Water mediated and Baker's yeast accelerated novel synthetic protocols for tetrahydrobenzo[a] xanthene-11-ones and pyrazolo[3,4-b]quinolines, Synth. Commun. 51 (2021) 1963–1973, https://doi.org/10.1080/00397911.2021.1913606.
- [37] S.K. Das, M. Tahu, M. Gohain, D. Deka, U. Bora, Bio-based sustainable heterogeneous catalyst for ipso-hydroxylation of arylboronic acid, Sustain. Chem. Pharm. 17 (2020) 100296, https://doi.org/10.1016/j.scp.2020.100296.
- [38] K. Laskar, P. Bhattacharjee, M. Gohain, D. Deka, U. Bora, Application of bio-based green heterogeneous catalyst for the synthesis of arylidinemalononitriles, Sustain. Chem. Pharm. 14 (2019) 100181, https://doi.org/10.1016/j.scp.2019.100181.
- [39] S. Thangadurai, J.T. Abraham, A.K. Srivastava, M. Nataraja Moorthy, S.K. Shukla, Y. Anjaneyulu, X-ray powder diffraction patterns for certain β-lactam, tetracycline and macrolide antibiotic drugs, Anal. Sci. 21 (2005) 833–838, https://doi.org/10.2116/analsci.21.833.
- [40] M. Sulpizi, G. Folkers, U. Rothlisberger, P. Carloni, L. Scapozza, Applications of density functional theory-based methods in medicinal chemistry, Quant. Structure-Activity Relatsh. 21 (2002) 173–181, https://doi.org/10.1002/1521-3838 (200207)21:2<173::AID-QSAR173>3.0.CO;2-B.
- [41] Z. Bayat, S. Vahdani, A simple and readily integratable approach to toxicity prediction for some of the anti cancer drugs, J. Chem. Pharm. Res. 3 (2011) 03 102
- [42] S. Murugavel, S. Sundramoorthy, D. Lakshmanan, R. Subashini, P. Pavan Kumar, Synthesis, crystal structure analysis, spectral (NMR, FT-IR, FT-Raman and UV-vis) investigations, molecular docking studies, antimicrobial studies and quantum chemical calculations of a novel 4-chloro-8-methoxyquinoline-2(1H)-one: an effective antimicrobial agent and an inhibition of DNA gyrase and lanosterol-14αdemethylase enzymes, J. Mol. Struct. 1131 (2017) 51–72, https://doi.org/ 10.1016/i.molstruc.2016.11.035.
- [43] P. Politzer, J.S. Murray, Molecular Electrostatic Potentials: significance and Applications 7.1 A Quick Review of Some Classical Physics, (2021) 113–134.
- [44] I. Hdoufane, J. Stoycheva, A. Tadjer, D. Villemin, M. Najdoska-Bogdanov, J. Bogdanov, D. Cherqaou, QSAR and molecular docking studies of indole-based analogs as HIV-1 attachment inhibitors, J. Mol. Struct. 1193 (2019) 429–443, https://doi.org/10.1016/j.molstruc.2019.05.056.
- [45] R. Srivastava, S.K. Gupta, F. Naaz, P.S. Sen Gupta, M. Yadav, V.K. Singh, A. Singh, M.K. Rana, S.K. Gupta, D. Schols, R.K. Singh, Alkylated benzimidazoles: design, synthesis, docking, DFT analysis, ADMET property, molecular dynamics and activity against HIV and YFV, Comput. Biol. Chem. 89 (2020) 107400, https://doi.org/10.1016/j.compbiolchem. 2020. 107400